Adsorption of industrial Acid Red 114 onto Fe$_3$O$_4$@Histidine magnetic nanocomposite

A. Yıldız[a,*], E. Güneş[b], Md. Amir[c], A. Baykal[c]

[a]*Department of Textile Engineering, Namık Kemal University, 59860 Çorlu-Tekirdağ, Tel. 90 (0282) 250 - 2326; email: ayildiz@nku.edu.tr*
[b]*Department of Environmental Engineering, Namık Kemal University, 59860 Çorlu-Tekirdağ, email: egunes@nku.edu.tr*
[c]*Department of Chemistry, Fatih University, 34500 B.Çekmece-İstanbul/Turkey, email: hadibaykal@gmail.com (Md. Amir), mdamir01031001@gmail.com (A. Baykal)*

ABSTRACT

Fe$_3$O$_4$@Histidine (Fe$_3$O$_4$@His) magnetic nanocomposite (MNCs) was successfully prepared by simple thermal decomposition method. The final obtained products were characterized by X-ray diffraction (XRD), Fourier transform infrared (FT-IR), thermogravimetric analysis, scanning electron microscope (SEM), and transmission electron microscopy (TEM). Powder XRD analysis confirmed the single phase of Fe$_3$O$_4$ spinel structure. SEM and TEM analysis indicated that Fe$_3$O$_4$@His MNCs were nanoparticles-like structure with small agglomeration. FT-IR results revealed that L-histidine made a bond through its COO$^-$ group with Fe$_3$O$_4$ Nanoparticles (NPs). There is electrostatic attraction between cationic NH$_2$ group (NH$_3^+$) of Fe$_3$O$_4$@His MNCs and anionic dye. The Fe$_3$O$_4$@His MNC has much higher adsorbed amount of Acid Red 114 (AR114) than the Fe$_3$O$_4$ NPs at pH 5 and 8. At pH –5 on the nanoparticle surface via ammonium groups. Thermal analysis showed the decomposition of the L-histidine capping. The hysteresis (σ–H) curves revealed Fe$_3$O$_4$@His MNC exhibit a typical super paramagnetic characteristic with a saturation magnetization of 45.5 emu/g. The adsorption capacity of low-cost and eco-friendly adsorbents Fe$_3$O$_4$@His nanocomposite for removal of industrial AR114 from wastewater was investigated. Therefore, pH of 5 and contact time of 120 min were found to be optimum for maximum removal of AR114 by Fe$_3$O$_4$@His MNCs. The experimental data of adsorption obey Langmuir isotherm and pseudo-second-order kinetic. The maximum adsorption capacity of the Fe$_3$O$_4$@His MNC for AR114 was 140.8 mg/g at pH 5. The reusability of the Fe$_3$O$_4$@His MNCs was also done, and significant removal of AR114 obtained even after five cycles. Thus, Fe$_3$O$_4$@His MNCs considered as a good stability and reusability absorbent for the removal of industrial AR114.

Keywords: Wastewater treatment; Magnetic nanocomposite; Adsorption; Acid Red 114

1. Introduction

The application of magnetic nanomaterials in dye wastewater treatment has received wide attention in recent years due to high adsorption rate, easy removal and recyclability [1].

Among these magnetic nanomaterials, magnetite (Fe$_3$O$_4$) based ones have drawn considerable attention because of its high surface area, low toxicity, low cost, eco-friendliness, easy separation and high reusability [2]. The important drawback of magnetic nanocomposite (MNC) usage for environmental pollution is the easy aggregation of magnetic nanomaterials, which limits its wide applications. To overcome this problem, to modify the surface of the magnetic material with coating is a good strategy to enhance the stability of composite material and adsorption ability.

Chang et al. synthesized the Fe$_3$O$_4$/activated montmorillonite (Fe$_3$O$_4$/Mt) nanocomposite via a coprecipitation method

* Corresponding author.

and evaluated the adsorption capacity of Fe_3O_4/Mt for methylene blue (MB). They found out that over 83.73% color removal of MB was obtained after five cycles [3]. In another study, Cao et al. studied the high adsorption capacity of magnetic Fe_3O_4/chitosan nanoparticles and removal rate of it for brilliant red (X-3B) [4]. Yao et al. used porous magnetic polyacrylamide microspheres for removal of industrial cationic dyes. These prepared microspheres showed a significant adsorption capacity of 1990 mg/g [5]. L-cysteine coated iron oxide magnetic nanoparticles (Cys–Fe_3O_4 MNPs) were synthesized by a simple high-gravity reactive precipitation method and used for the heavy metal adsorption (Pb(II) and Cd(II)) by Fan et al. [6]. Song et al. synthesized the amine functionalized Fe_3O_4 magnetic biopolymer resin 10 (amine/Fe_3O_4-resin) and used and applied for the removal of some anionic dyes from wastewater [7]. Mesoporous graphene/Fe_3O_4/chitosan nanocomposite was also used for the adsorption capacity for a textile dye (MB) and found out that the adsorption capacity reached 98% within a contact time of 5 min at pH 9 and an initial dye concentration of 25 mg/L [8]. Wang et al. functionalized the Fe_3O_4 nanoparticles with SiO_2 which was further functionalized with thiol (–SH) group and used for Hg(II) adsorption [9]. Zhang et al. used the humic acid-coated Fe_3O_4 nanoparticles for the adsorption of MB and studied on the desorption process also [10]. Safavi and Momeni synthesized a nanocatalyst of palladium/hydroxyapatite/Fe_3O_4 (Pd/HAP/Fe_3O_4) and studied briefly the catalytic activity of this newly prepared toward the degradation of methyl red, methyl orange and methyl yellow [11]. Chong et al. successfully synthesized the magnetic FeO/Fe_3O_4/graphene by a one-step reduction method and investigated in rapid degradation of dyes. After 20 min of reaction, the removal efficiencies of methyl orange, MB and 547 crystal violet were 94.78%, 91.60% and 89.07%, respectively [12]. Tan et al. used the activated maize cob impregnated with magnetic nanoparticles (Fe_3O_4 nanoparticles) for MB adsorption [13] and found out that the optimum efficiency of MB dye removal was 99.63%.

Many techniques were done on removal of aqueous dyes from the wastewater of textiles effluents such as conventional physicochemical, biological treatment, photocatalytic method and so on that are not completely beneficial for their removal due to high cost of processing, required wide area of land to treat large amount of dye wastewaters [14]. Among them, adsorption is more advanced physical and chemical treatment for removing these pollutants [15]. Among these dyes pollutants, Acid Red 114 (AR114) reported as more toxics and need to be taken out often from the industrial wastewater, as for example Manouchehr et al. studied on the removal of AR114 by photocatalytic techniques in water with TiO_2 supported catalyst [16]. Lin and Thinkarin were also reported on the removal of AR114 by different techniques [17,18]. However, none of the studies reported on the remediation of AR114 by adsorption method.

This work reported low-cost and eco-friendly adsorbent Fe_3O_4@Histidine (Fe_3O_4@His) MNCs, for the complete removal of AR114 aqueous pollutants from the industrial wastewater by an easy and more conventional adsorption method, and its stability and recyclability were also done.

2. Experimental setup

2.1. Chemicals

Iron (III) chloride hexahydrate, iron (II) chloride tetrahydrate, l-histidine, ammonia solution, acetic acid, sodium hydroxide, methanol, HCl and C.I. AR114 were taken from Merck (Darmstadt, Germany) and used without further purification.

2.2. Instrumentations

Powder X-ray diffraction (XRD) analysis was conducted on a Huber JSODebyeflex 1001 diffractometer operated at 40 kV and 35 mA using Cu Kα radiation.

Fourier transform infrared (FT-IR) spectra were recorded in transmission mode with a PerkinElmer BX FT-IR infrared spectrometer. The powder samples were ground with KBr and compressed into a pellet. FT-IR spectra in the range 4000–400 cm^{-1} were recorded in order to investigate the nature of the chemical bonds formed.

Transmission electron microscopy (TEM) analysis was performed using an FEI Tecnai G2 Sphera microscope. A drop of diluted sample in alcohol was dripped on a TEM grid.

Zeta potential and particle size measurements were performed using a particle size analyzer (Brookhaven Instruments, New York) in folded capillary zeta potential cells, and pH titrations were performed using 0.05 M NaOH and 0.05 M HCl.

The thermal stability was determined by thermogravimetric analysis (TGA; PerkinElmer Instruments model, STA 6000). The TGA thermograms were recorded for 5 mg of powder sample at a heating rate of 10°C/min. in the temperature range of 30°C–800°C under nitrogen atmosphere.

Thermo Spectronic AquaMate Visible Light spectrophotometer has 315–1100 nm wavelength range.

Biosan PSU-10i Orbital Shaker was used to stir Fe_3O_4@His MNC with AR114.

2.3. Synthesis

The preparation of Fe_3O_4@His MNCs has been already reported in our previous report [19,20]. Briefly, the salts of FeCl3.2H$_2$O and FeCl$_2$.4H$_2$O were taken in the molar ratio of 2:1 with 0.5 g of L-histidine and dissolved in 50 ml of distilled water in three-neck round-bottom flask. Then their homogeneous solutions were prepared using magnetic stirring at 40°C for 15 min under vigorous stirring. Then NH$_3$ solution was added drop wise till the pH was raised to ~11 at which the precipitation of all ferrites takes place. This black precipitate was then refluxed at 80°C for 6 h with constant stirring and under influence of Argon gas. Finally, Fe_3O_4@His MNCs were separated from the aqueous solution by magnetic decantation and washed with distilled water several times, and at the end, it kept inside the oven at 80°C for 12 h [21–32].

2.4. Adsorption studies

In the present study, AR114 ($C_{37}H_{28}N_4O_{10}S_3Na_2$, 830 g/mol) was chosen as an adsorbate because it is a dye contaminant in discharged effluents [17]. The aqueous solution of AR114 (200 mg/L) was prepared at pH 7, and then other

AR114 solutions with the required concentrations were prepared by successive dilution of this stock solution. The effect of pH of solution on adsorption was studied by performing related experiments at five different pH of 3, 5, 8, 10 and 12 for which 1 M HCI and 1 M NaOH were used. For the adsorption studies, 10, 20, 40, 60 and 80 mg/L dye concentrations were used to investigate the adsorptive capacity of adsorbent, and the effects of contact time (0, 1, 5, 10, 15, 30, 45, 60, 90 and 120 min) on color removal were also studied by a series of kinetic experiments which were carried out at fixed adsorbent dosage (0.01 g/50 mL) in the aqueous solution at room temperature. A control flasks containing only the adsorbent in 50 mL of deionized water was used simultaneously under the same conditions. The prepared solution in each flask was agitated at 200 rpm for 2 h, and supernatant was centrifuged at 4000 rpm for 5 min, and then the absorbance of AR114 in the supernatant was measured. The absorbance values of dye solutions were measured at $\lambda = 522$ nm at which AR114 has the maximum absorbance.

The amount of adsorbed AR114 was calculated from the following equation:

$$q_e = V (C_0 - C_e) / W \tag{1}$$

where q_e is the amount adsorbed (mg/g); C_0 and C_e are the initial and equilibrium AR114 concentrations in the solution (mg/L), respectively; V is the solution volume (L) and W is the mass of adsorbent (g).

The rate of the sorption is considered as one of the important factors while analyzing the efficiency of sorption [33]. The adsorption kinetics were investigated to better understand the dynamics of the adsorption processes [34].Therefore, we done the experiments by using Fe_3O_4@His MNC to assess the kinetics of AR114 removal from wastewater. Additionally, Langmuir and Freundlich isotherm models were applied to determine the adsorption capacity of the adsorbents (Fe_3O_4@ His MNCs).

2.5. Regeneration and reuse experiments

The recycling and regeneration ability is significant for the practical application of adsorbents since they must possess high desorption efficiency as well as higher adsorption capacity which allows the reduction of overall cost of the adsorbent. Thus, desorption experiments of Fe_3O_4@His MNCs were also performed to evaluate the recyclability of Fe_3O_4@His MNCs. Desorption experiments were conducted as follows: 0.01 g of AR114-loaded adsorbents were added to 50 mL of a mixture of methanol and acetic acid (volume ratio of 9:1) [35]. The 5 g of Fe_3O_4@His MNC was added into the 1-L mixture of methanol and acetic acid, and the Fe_3O_4@His MNC was shaken for 1 h to reach desorption equilibrium. After regeneration, Fe_3O_4@His MNC was separated with an external magnet, and the AR114 concentration in liquid was measured with a Thermo Spectronic AquaMate spectrometer at 522 nm to estimate the desorbed amount of AR114. The same step was repeated for three times until the AR114 concentration in the liquid was lower than 0.002 mmol/L [35]. Then the NPs were washed with ultrapure water and air-dried in oven. The adsorption/desorption of the AR114 from the His-Fe_3O_4 NPs were assessed in five consecutive cycles (Fig. 1).

3. Results and discussion

The complete characterization of Fe_3O_4@His MNCs has been already given in our previous report [19].

3.1. Comparison of AR114 adsorption onto Fe_3O_4@His MNCs and Fe_3O_4 NPs

To compare adsorption capacity of Fe_3O_4@His MNC and Fe_3O_4 NPs, acidic (pH 5) and basic conditions (pH 8) were studied. Comparison of AR114 adsorption onto Fe_3O_4@His MNC and Fe_3O_4 NPs is given in Fig. 2, which showed that there are differences between Fe_3O_4 NPs and Fe_3O_4@His MNC adsorption capacity. The Fe_3O_4@His MNC has much higher adsorbed amount of AR114 than the Fe_3O_4 NPs at pH 5 and pH 8. At pH 5, Fe_3O_4@His MNCs has about 114 mg/g q_e AR114 adsorption. The reason for the higher adsorption rate (higher q_e) of Fe_3O_4@His MNCs than Fe_3O_4 NPs has may be the formation of the activated sites on the surface of Fe_3O_4@ His MNCs for the adsorption of AR114.

3.2. Influence of solution pH on adsorption of AR114 on Fe_3O_4@His MNCs

To examine the effect of pH on the adsorption of AR114 by Fe_3O_4@His MNCs from aqueous solutions, the adsorption experiments were carried out at pH 3, 5, 8, 10 and 12 with 0.01 g/L dosage of an Fe_3O_4@His MNCs with an initial AR114 concentration of 40 mg/L (Fig. 3). It is seen from Fig. 3 that the adsorbent showed better adsorption capacity at the pH of 5. As it is seen from Fig. 3, the q_e values increased from 54 to 114 mg/g when the pH is increased from 3 to 5 and it is decreased to 13 mg/g for pH is equal to 12. As it is reported, Fe_3O_4 NPs can easily oxidized and hence quickly lost their magnetism or even dissolved when pH was below 4.0 [35]. A similar result was observed for the adsorption of AR114 in this study also. AR114 is polar molecule ($R-SO_3^{2-}$) at low pH [33]. The pH of the isoelectric point of Fe_3O_4 is approximately 5.9, and the surface charge of Fe_3O_4 is positive at pH < 5.9 [18]. Therefore, the electrostatic interaction between the surface of Fe_3O_4@His MNC and the anionic AR114 molecules promoted the adsorption of AR114 at pH < 5.9. It showed that while increasing pH of the system, the total number of negative charged sites is also increased [35]. Therefore, the adsorption of AR114 molecules which is an anionic dye decreases when pH > 5 as it is shown in Fig. 3.

3.3. Adsorption isotherms

At constant temperature, the term adsorption isotherm is known as the equilibrium relationship of quantity of adsorbate per unit of adsorbent (q_e) and the equilibrium solution concentration of absorbent [36]. Initial dye concentrations of 10, 20, 40, 60 and 80 mg/L were used for isotherm studies and to investigate the adsorptive capacity of adsorbent at pH 5, adsorbent dosage of 0.01 g/50 mL and equilibrium time of 120 min. In this study, common isotherm models of Freundlich and Langmuir were employed to describe the equilibrium characteristics of adsorption [37–39]. The linearized equation of Langmuir is represented according to Eq. (2) [40]:
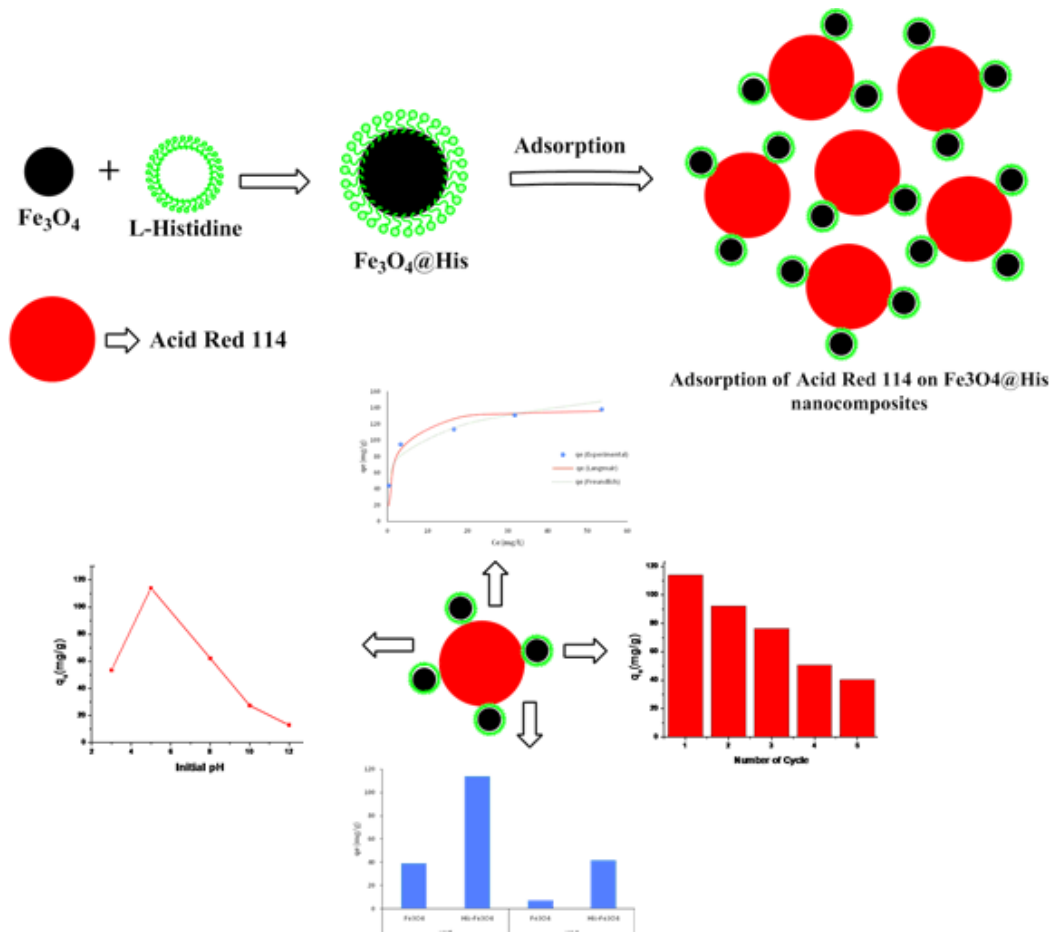
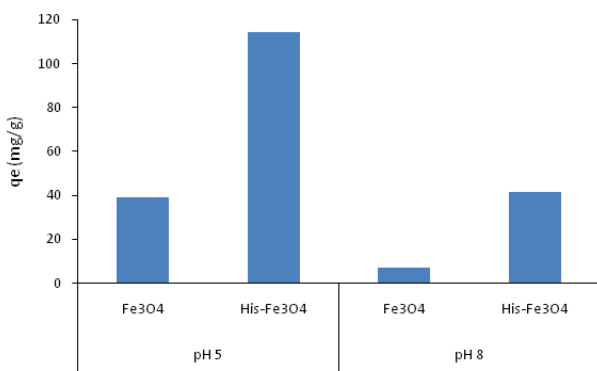Fig. 1. The schematic representation of removal of Acid Red 114 on the Fe$_3$O$_4$@His MNCs.

Fig. 2. Comparison of AR114 adsorption onto Fe$_3$O$_4$@His MNCs and Fe$_3$O$_4$ NPs at pH 5 and at pH 8 (initial dye concentration: 40 mg/L, t: 120 min, adsorbent dose: 0.2 g/L).

Fig. 3. Influence of initial pH on adsorption onto Fe$_3$O$_4$@His MNCs (initial dye concentration: 40 mg/L, t: 120 min, adsorbent dose: 0.2 g/L).

$$\frac{C_e}{q_e} = \frac{1}{q_{max}} C_e + \frac{1}{q_{max} K_L} \qquad (2)$$

where q_e (mg/g) is the amount of AR114 adsorbed per unit mass of adsorbent particles at equilibrium; C_e (mg/L) is the equilibrium liquid concentration of AR114; K_L is the
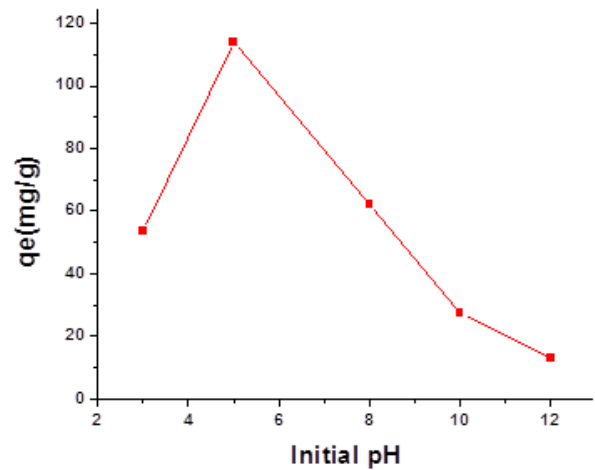
equilibrium constant (L/mg); and q_{max} is the amount of adsorbate required to form monolayer and maximum adsorption capacity (mg/g). The experimental data are then fitted into the above equation for linearization by plotting

C_e/q_e against C_e. From the data of C_e/q_e against C_e, q_{max} and K_L values can be determined.

The linearized Freundlich equation is given according to Eq. (3) [41]. The factors affecting adsorption capacity and intensity of the adsorption process are K_f and n. Here n and K_f can be calculated from the slope and intercept, respectively.

$$\log q_e = \log K_f + n \log C_e \tag{3}$$

Table 1 summarizes the correlation coefficients for the two isotherms such as the K_f and n values for the Freundlich isotherm and the q_{max} and K_L values for the Langmuir isotherm. As it is seen from R^2 values given in Table 1, the Langmuir equation yielded the best fit to the experimental data in comparison with Freundlich equation in this study.

Table 1
Adsorption isotherm parameters of AR114 onto Fe_3O_4@His MNC by Langmuir and Freundlich equations

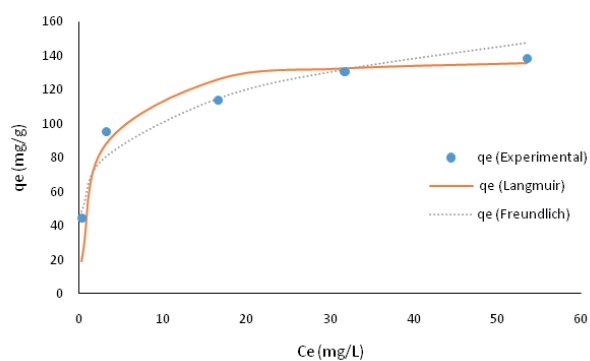| Langmuir isotherm			Freundlich isotherm		
q_{max} (mg/g)	K_L (L/mg)	R^2	n	K_f (mg/g)	R^2
140.8	0.526	0.9964	4.67	62.9	0.9534

Fig. 4. Adsorption isotherms of AR114 onto Fe_3O_4@His MNCs (pH: 5, t: 120 min, initial dye concentration: 10, 20, 40, 60, 80 mg/L, adsorbent dose:0.2 g/L).

Langmuir model is generally based on uniform, monolayer and finite adsorption site assumptions [40]. As can be seen from Table 1, the maximum adsorption capacity (q_{max}) of Fe_3O_4@His MNCs is 140.8 mg/g for adsorption of AR114 on Fe_3O_4@His MNCs. It can be understood that it possesses good adsorption capacity for AR114 dye compared with activated carbons prepared from agricultural waste materials [34]. Values of $n > 1$ represent a favorable adsorption process. As it is seen from Table 1, that n was calculated as 4.67, which represent a favorable adsorption process for AR114 onto Fe_3O_4@His MNC. The experimental data and the fitted isotherms of AR114 adsorption onto Fe_3O_4@His MNC were represented in Fig. 4.

Table 2 gives the q_{max} values obtained in this study in comparison with the q_{max} values obtained in the other studies carried out with various MNCs. As you seen from Table 2, Fe_3O_4@His have suitable adsorption capacity with regard to the removal of AR114.

3.4. Adsorption kinetics

The rate of the sorption is considered as one of the important factors while analyzing the efficiency of sorption [32]. For kinetic study, contact time of 0, 1, 5, 10, 15, 30, 45, 60, 90 and 120 min were studied at adsorbent dosage of 0.01 g/50 mL, initial dye concentration of 40 mg/L, pH 5 and room temperature. Adsorption mechanism and kinetics of AR114 adsorption onto Fe_3O_4@His MNC were analyzed using pseudo-first-order and pseudo-second order models. Pseudo-first-order kinetics equation can be expressed as follows (Eq. (4)) [42]:

$$\log(q_e - q_t) = \log q_e - \frac{k_1}{2.303} t \tag{4}$$

where q_e is known as the amount adsorbed (mg/g) at equilibrium, while q_t is the amount adsorbed (mg/g) at time t, and k_1 is the pseudo-first-order adsorption rate coefficient (min^{-1}). The values of $q_{e,calc}$ and k_1 were determined from linear plots of $\log(q_e - q_t)$ vs t (Fig. 5(a)). Pseudo-second-order kinetics equation can be expressed as follows (Eq. (5)) [42]:

$$\frac{t}{q_t} = \frac{1}{k_2 q_e^2} + \frac{t}{q_e} \tag{5}$$

Table 2
Adsorption capacities obtained from present study and other studies for the removal of AR114 and various pollutants

Adsorbent	Pollutant	Q_{max} (mg/g)	Reference
Commercial activated carbon	Acid Yellow 23	56.5	[17]
Activated pongam seed shells	AR114	204	[17]
Activated cotton seed shells	AR114	153	[17]
Activated sesame seed shells	AR114	102	[17]
RPB-Fe_3O_4	Reactive Red 2	97.8	[18]
Fe_3O_4/graphene	Bisphenol A	72.80	[34]
HA-Fe_3O_4	Methylene blue	93	[35]
Fe_3O_4@His	AR114	140	This study
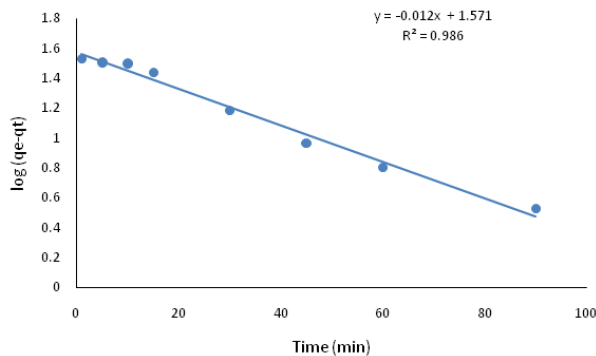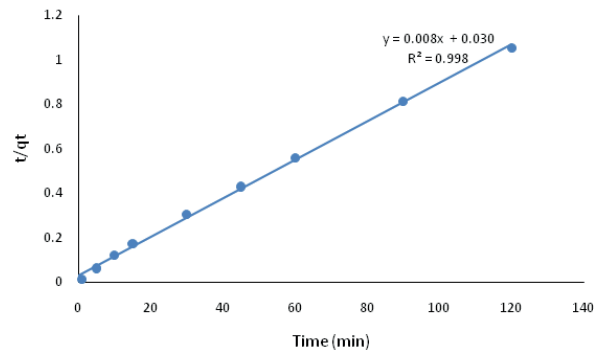
Fig. 5. Plot of pseudo-first-order (a) and second-order (b) equation for adsorption of AR114 onto Fe$_3$O$_4$@His MNCs (pH: 5, initial dye concentration: 40 mg/L, adsorbent dose: 0.2g/L).

where k_2 (g/mg min) is the second-order rate constant while q_t (mg/g) is the amount of dye adsorbed at a certain time t (min). The values of $q_{e,calc}$ and k_2 were determined from linear plots of t/q_t vs. t (Fig. 5). As it is seen from Figs. 5(a) and (b), the values of R^2 for the first-order model and the second-order model were 0.9866 and 0.9984, respectively. The R^2 obtained from the second-order model is higher than from the first-order model indicating the suitability of the second-order model. By looking these results, it can be concluded that the rate of sorption is dependent on the availability of the sorption sites and independent of the concentration of the sorbate in the bulk solution [43]. Equilibrium adsorption capacity, $q_{e,calc}$, was calculated by using the second-order model. $q_{e,calc}$ of the Fe$_3$O$_4$@His MNCs was found as 114.9 mg/g which showing a good agreement with the experimental value ($q_{e,exp}$ = 114.03 mg/g).

3.5. Regeneration and reuse

Potential industrial application of any adsorbent is based on its stability and regeneration ability. In order to reduce the overall cost of the adsorbent, the adsorption efficiency and regeneration potential of Fe$_3$O$_4$@His MNC was investigated. The adsorbed AR114 was released easily from Fe$_3$O$_4$@His MNC adsorbent by shaking in a mixture of acetic acid and methanol. The absorbent was separated by magnet and reused. The recycling adsorption efficiency is shown in Fig. 6 from which the adsorbed amount of AR114 onto the Fe$_3$O$_4$@His MNC was 114 mg/g, and the adsorbed amount of AR114 onto the regenerated Fe$_3$O$_4$@His MNC decreased each cycle from 114 to 40 mg/g.

4. Conclusion

L-histidine coated Fe$_3$O$_4$ MNCs were synthesized successfully by the simple chemical refluxed method. This study showed that magnetic nanomaterials supported adsorbent are very attractive and may be a good alternative solution for wastewater treatment due to its very efficient adsorbent capability and stability for reusable adsorbing materials used in the removal of hazardous dye. This work also showed that
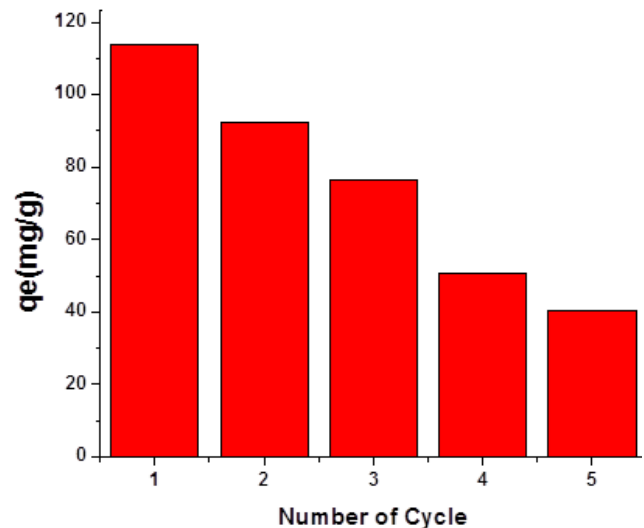

Fig. 6. Recyclability of Fe$_3$O$_4$@His MNC.

this l-histidine capped Fe$_3$O$_4$ MNCs has suitable adsorption ability toward the removal of AR114 from the wastewater. The effect of pH was investigated at pH 3, 5, 8, 10 and 12. At pH 5 which the maximum dye removal were obtained and at 120 min which equilibrium time was obtained, initial dye concentrations of 10, 20, 40, 60 and 80 mg/L were used for equilibrium studies and to investigate the adsorptive capacity of adsorbent. The effects of contact time (0, 1, 5, 10, 15, 30, 45, 60, 90 and 120 min) on dye removal were also studied by a series of kinetic experiments, which were carried out at fixed adsorbent dosage (0.01 g/50 mL) and initial dye concentration of 40 mg/L in the aqueous solution at room temperature. The maximum adsorption capacity of the Fe$_3$O$_4$@His MNC for AR114 was calculated from Langmuir isotherm model as 140.8 mg/g. Adsorption results obey both Langmuir and Freundlich isotherms. From R^2 values given the Langmuir equation yielded the best fit to the experimental data. Its kinetics study follows pseudo-second-order rate expression, which fits best for this study. This MNCs works well as an

adsorbents are easy to synthesize by the help of available materials. Finally, Fe₃O₄@His MNC can be considered as an alternatives and efficient adsorbents for dye removal in wastewater treatment.

References

[1] K.B. Tan, M. Vakili, B.A. Horri, P.E. Poh, A.Z. Abdullah, B. Salamatinia, Adsorption of dyes by nanomaterials: recent developments and adsorption mechanisms, Sep. Purif. Technol., 150 (2015) 229–242.

[2] Q. Zhoua, Y. Wan, J. Xiao, H. Fan, Adsorption and removal of bisphenol A, a-naphthol and b-naphthol from aqueous solution by Fe₃O₄@polyaniline core–shell nanomaterials, Synth. Met., 212 (2016) 113–122.

[3] J. Chang, J. Ma, Q. Ma, D. Zhang, N. Qiao, M. Hu, H. Ma, Adsorption of methylene blue onto Fe₃O₄/activated montmorillonite nanocomposite, Appl. Clay Sci., 119 (2016) 132–140.

[4] C. Cao, L. Xiao, C. Chen, X. Shi, Q. Cao, L. Gao, In situ preparation of magnetic Fe₃O₄/chitosan nanoparticles via a novel reduction–precipitation method and their application in adsorption of reactive azo dye, Powder Technol., 260 (2014) 90–97.

[5] T. Yao, S. Guo, C. Zeng, C. Wang, L. Zhang, Investigation on efficient adsorption of cationic dyes on porous magnetic polyacrylamide microspheres, J. Hazard. Mater., 292 (2015) 90–97.

[6] H.L. Fan, L. Lia, S.F. Zhou, Y.Z. Liu, Continuous preparation of Fe₃O₄ nanoparticles combined with surface modification by L-cysteine and their application in heavy metal adsorption, Ceram. Int., 42 (2016) 4228–4237.

[7] W. Song, B. Gao, X. Xu, L. Xing, S. Han, P. Duan, W. Song, R. Jia, Adsorption desorption behavior of magnetic amine/Fe₃O₄ functionalized biopolymer resin towards anionic dyes from wastewater, Bioresour. Technol., 210 (2016) 123–130. doi: 10.1016/j.biortech.2016.01.078

[8] N.V. Hoa, T.T. Khong, T.T.H. Quyen, T.S. Trung, One-step facile synthesis of mesoporous graphene/Fe₃O₄/chitosan nanocomposite and its adsorption capacity for a textile dye, J. Water Process. Eng., 9 (2016) 170–178.

[9] Z. Wang, J. Xu, Y. Hu, H. Zhou, J. Zhou, Y. Liu, A. Lou, X. Xu, Functional nanomaterials study on aqueous Hg(II) adsorption by magnetic Fe₃O₄@SiO₂-SH nanoparticles, J. Taiwan Inst. Chem. Eng., 60 (2015) 394–402. doi: 10.1016/j.jtice.2015.10.041

[10] X. Zhang, P. Zhang, Z. Wu, L. Zhang, G. Zeng, C. Zhou, Adsorption of methylene blue onto humic acid-coated Fe₃O₄ nanoparticles, Colloids Surf., A, 435 (2013) 85–90.

[11] A. Safavi, S. Momeni, Highly efficient degradation of azo dyes by palladium/hydroxyapatite/Fe₃O₄ nanocatalyst, J. Hazard. Mater., 201–202 (2012) 125–131.

[12] S. Chong, G. Zhang, H. Tian, H. Zhao, Rapid degradation of dyes in water by magnetic Fe₀/Fe₃O₄/graphene composites, J. Environ. Sci., 44 (2016) 148–157. doi: 10.1016/j.jes.2015.11.022

[13] K.A. Tan, N. Morad, T.T. Teng, I. Norli, Synthesis of magnetic nanocomposites (AMMC - Fe₃O₄) for cationic dye removal: optimization, kinetic, isotherm, and thermodynamics analysis, J. Taiwan Inst. Chem. Eng., 54 (2015) 96–108.

[14] R.S. Juang, R.L. Tseng, F.C. Fu, Use of chitin and chitosan in lobster shell wastes for colour removal from aqueous solutions, J. Environ. Sci. Health., Part A, 31 (1996) 325–338.

[15] P. Cooper, Removing colour from dye house wastewaters – a critical review of technology available, J. Soc. Dyers Colourists, 109 (1993) 97–101.

[16] M. Nikazar, K. Gholivandb, K. Mahanpoor, Photocatalytic degradation of azo dye Acid Red 114 in water with TiO₂ supported on clinoptilolite as a catalyst, Desalination, 219 (2008) 293–300.

[17] N. Thinakaran, P. Panneerselvam, P. Baskaralingam, D. Elango, S. Sivanesan, Equilibrium and kinetic studies on the removal of Acid Red 114 from aqueous solutions using activated carbons prepared from seed shells, J. Hazard. Mater., 158 (2008) 142–150.

[18] C.C. Lin, Y.S. Lin, J.M. Ho, Adsorption of Reactive Red 2 from aqueous solutions using Fe₃O₄ nanoparticles prepared by co-precipitation in a rotating packed bed, J. Alloys Compd., 666 (2016) 153–158.

[19] B. Ünal, Z. Durmus, A. Baykal, H. Sözeri, M.S. Toprak, L. Alpsoy, L-histidine coated iron oxide nanoparticles: synthesis, structural and conductivity characterization, J. Alloys Compd., 505 (2010) 172–178.

[20] A. Baykal, Md. Amir, S. Güner, H. Sözeri, Preparation and characterization of SPION functionalized via caffeic acid, J. Magn. Magn. Mater, 395 (2015) 199–204.

[21] B. Unal, M.S. Toprak, Z. Durmus, H. Sözeri, A. Baykal, Synthesis, structural and conductivity characterization of alginic acid - Fe₃O₄ nanocomposite, J. Nanopart. Res., 12 (2010) 3039–3048.

[22] L.J. Kirwan, P.D. Fawell, W.V. Bronswijk, In situ FTIR-ATR examination of poly(acrylic acid) adsorbed onto hematite at low pH, Langmuir, 19 (2003) 5802–5807.

[23] Z. Durmus, H. Kavas, M.S. Toprak, A. Baykal, T.G. Altınçekiç, A. Aslan, A. Bozkurt, S. Coşgun, L-lysine coated iron oxide nanoparticles: synthesis, structural and conductivity characterization, J. Alloys Compd., 484 (2009) 371–376.

[24] Z. Durmus, H. Kavas, A. Baykal, H. Sozeri, L. Alpsoy, S.Ü. Çelik, M.S. Toprak, Synthesis and characterization of l-carnosine coated iron oxide nanoparticles, J. Alloys Compd., 509 (2011) 2555–2561.

[25] T. Özkaya, M.S. Toprak, A. Baykal, H. Kavas, Y. Köseoğlu, B. Aktaş, Synthesis of Fe₃O₄ nanoparticles at 100°C and its magnetic characterization, J. Alloys Compd., 472 (2009) 18–23.

[26] A.M. Petrosyan, Vibrational spectra of L-histidine perchlorate and L-histidine tetrafluoroborate, Vib. Spectrosc., 43 (2007) 284–289.

[27] J.Y. Park, E.S. Choi, M.J. Baek, G.H. Lee, Colloidal stability of amino acid coated magnetite nanoparticles in physiological fluid, Mater. Lett., 63 (2009) 379–381.

[28] J.A. Kieft, K. Nakamoto, Infrared spectra of some platinum(II) glycine complexes, J. Inorg. Nucl. Chem., 29 (1967) 2561–2568.

[29] U. Kurtan, Md. Amir, A. Baykal, Fe₃O₄@Nico-Ag magnetically recyclable nanocatalyst for azo dyes reduction, Appl. Surf. Sci., 363 (2016) 66–73.

[30] Md. Amir, U. Kurtan, A. Baykal, Rapid color degradation of organic dyes by Fe₃O₄@His@Ag recyclable magnetic nanocatalyst, J. Ind. Eng. Chem., 27 (2015) 347–353.

[31] A. Baykal, Md. Amir, S. Güner, H. Sözeri, Preparation and characterization of SPION functionalized via caffeic acid, J. Magn. Magn. Mater, 395 (2015) 199–204.

[32] Md. Amir, U. Kurtan, A. Baykal, Synthesis and application of magnetically recyclable nanocatalyst Fe₃O₄@Nico@Cu in the reduction of azo dyes, Chinese J. Catal., 36 (2015) 1280–1286.

[33] S. Ayoob, A.K. Gupta, P.B. Bhakat, V.T. Bhat, Investigations on the kinetics and mechanisms of sorptive removal of fluoride from water using alumina cement granules, Chem. Eng. J., 140 (2008) 6–14.

[34] K. Ouyang, C. Zhu, Y. Zhao, L. Wang, S. Xie, Q. Wang, Adsorption mechanism of magnetically separable Fe₃O₄/grapheneoxide hybrids, Appl. Surf. Sci., 355 (2015) 562–569.

[35] X. Zhang, P. Zhang, Z. Wu, L. Zhang, G. Zeng, C. Zhou, Adsorption of methylene blue onto humic acid-coated Fe₃O₄ NPs, Colloids Surf., A, 435 (2013) 85–90.

[36] M. Iram, C. Guoa, Y. Guan, A. Ishfaq, H.L. Huizhou, Adsorption and magnetic removal of neutral red dye from aqueous solution using Fe₃O₄ hollow nanospheres, J. Hazard. Mater., 181 (2010) 1039–1050.

[37] A. Mittal, V. Thakur, J. Mittal, H. Vardhan, Process development for the removal of hazardous anionic azo dye Congo Red from wastewater by using hen feather as potential adsorbent, Desal. Wat. Treat., 52 (2014) 227–237.

[38] V.S. Mane, I.D. Mall, V.C. Srivastava, Kinetic and equilibrium isotherm studies for the adsorptive removal of Brilliant Green dye from aqueous solution by rice husk ash, J. Environ. Manage., 84 (2007) 390–400.

[39] S. Hashemian, H. Saffari, S. Ragabion, Adsorption of cobalt(II) from aqueous solutions by Fe_3O_4/bentonite nanocomposite, Water, Air, Soil Pollut., 226 (2014) 2212. doi: 10.1007/s11270-014-2212-6

[40] I. Langmuir, The adsorption of gases on plane surfaces of glass, mica and platinum, J. Am. Chem. Soc., 40 (1918) 1361–1403.

[41] H. Freundlich, Over the adsorption in solution, J. Phys. Chem., 57 (1906) 385–470.

[42] S. Lagergren, Zur Theorie der Sogenannten Adsorption Geloester Stoffe [About Theory of So-Called Adsorption of Soluble Substances], Kungliga Svenska Vetenskapsakad. Handl., 24 (1898) 1–39.

[43] M.U. Dural, L. Cavas, S.K. Papageorgiou, F.K. Katsaros, Methylene blue adsorption on activated carbon prepared from *Posidonia oceanica* (L.) dead leaves: kinetics and equilibrium studies, Chem. Eng. J., 168 (2011) 77–85.